ARL-TR-9826 ● Oct 2023

A Parametric Analysis of Dynamic Tensile Extrusion Using ALEGRA

by Matthew J Coppinger

NOTICES

Disclaimers

The findings in this report are not to be construed as an official Department of the Army position unless so designated by other authorized documents.

Citation of manufacturer's or trade names does not constitute an official endorsement or approval of the use thereof.

Destroy this report when it is no longer needed. Do not return it to the originator.

ARL-TR-9826 ● OCT 2023

A Parametric Analysis of Dynamic Tensile Extrusion Using ALEGRA

Matthew J Coppinger
DEVCOM Army Research Laboratory

REPORT DOCUMENTATION PAGE

1. REPORT DATE	2. REPORT TYPE	3. DATES COVERED	
		START DATE	END DATE
October 2023	Technical Report	5/01/2021	9/30/2023

4. TITLE AND SUBTITLE
A Parametric Analysis of Dynamic Tensile Extrusion Using ALEGRA

5a. CONTRACT NUMBER	5b. GRANT NUMBER	5c. PROGRAM ELEMENT NUMBER
5d. PROJECT NUMBER	**5e. TASK NUMBER**	**5f. WORK UNIT NUMBER**

6. AUTHOR(S)
Matthew J Coppinger

7. PERFORMING ORGANIZATION NAME(S) AND ADDRESS(ES)
DEVCOM Army Research Laboratory
ATTN: FCDD-RLA-TA
Aberdeen Proving Ground, MD 21005

8. PERFORMING ORGANIZATION REPORT NUMBER
ARL-TR-9826

9. SPONSORING/MONITORING AGENCY NAME(S) AND ADDRESS(ES)	10. SPONSOR/MONITOR'S ACRONYM(S)	11. SPONSOR/MONITOR'S REPORT NUMBER(S)

12. DISTRIBUTION/AVAILABILITY STATEMENT
DISTRIBUTION STATEMENT A. Approved for public release: distribution unlimited.

13. SUPPLEMENTARY NOTES

14. ABSTRACT
This parametric study uses a hydrocode to explore the effects of varying several dimensions and properties of dynamic tensile extrusion (DTE). A comparison is made to published data for the material models used. Then variations in the geometry of an extrusion die and properties of the projectile are examined. Comparisons are made regarding the peak and downrange velocities as individual DTE components are modified.

15. SUBJECT TERMS
dynamic tensile extrusion, ALEGRA, hydrocode, velocity enhancement, parametric study, Terminal Effects

16. SECURITY CLASSIFICATION OF:			17. LIMITATION OF ABSTRACT	18. NUMBER OF PAGES
a. REPORT	b. ABSTRACT	C. THIS PAGE		
UNCLASSIFIED	UNCLASSIFIED	UNCLASSIFIED	UU	23

19a. NAME OF RESPONSIBLE PERSON	19b. PHONE NUMBER *(Include area code)*
Matthew J Coppinger	(410) 278-0185

STANDARD FORM 298 (REV. 5/2020)
Prescribed by ANSI Std. Z39.18

Contents

List of Figures

List of Tables

Acknowledgments

This work was supported in part by a grant of computer time from the Department of Defense (DOD) High Performance Computing Modernization Program at the US Army Combat Capabilities Development Command Army Research Laboratory DOD Supercomputing Resource Center and the Terminal Ballistics Frontier project.

1. Introduction

The US Army Combat Capabilities Development Command (DEVCOM) Army Research Laboratory (ARL) recently developed and refined a method of delivering millimeter-sized pellets at hypervelocity for investigations in a laboratory setting.[1–5] Such technologies permit the rapid generation of a wealth of information concerning high-velocity material interactions. One approach to potentially achieve yet higher velocities involves leveraging a material analysis technique known as dynamic tensile extrusion (DTE). DTE involves extruding a projectile though a conical section of a die. The concept was originally conceived as means to probe the state of materials undergoing high strain rate tensile deformations.[6] A secondary effect of DTE is a velocity enhancement occurs during the process. This phenomenon has been reported in studies exploring the DTE of copper (Cu) and zirconium.[7,8] In addition, ARL developed a method of electrifying hemispherical nose aluminum projectiles during DTE with the intent of further increasing the velocity enhancement.[9]

Computational efforts have also explored DTE. Bonora et al. used modified Johnson–Cook (JC)[10] and Rusinek–Klepaczko[11] models to accommodate high strain rate effects and assess performance for the DTE of oxygen-free high conductivity (OFHC) Cu.[12] Burkett conducted hydrocode simulations to compare the performance of the mechanical threshold stress (MTS),[13] Zerrelli–Armstrong,[14] and JC[10] yield models with multiple sets of experimental data.[15] Further, Burkett considered velocity as a performance metric, and noted that the MTS model was able to reasonably capture the lead particle velocity of an extruded tantalum (Ta) specimen. These previous efforts focused on comparisons to existing experimental data; therefore, the effects of parametric changes to the extrusion die geometry were not evaluated.

In this report, a hydrocode is used to quantify the effect of changes in the extrusion die geometry on the downrange lead particle velocity and the peak velocity during extrusion. Additionally, velocity changes with variations in the projectile temperature, incoming velocity, and geometry are also considered. The results presented here highlight some potential benefits of parametric variations in the components of DTE as they pertain to maximizing velocity.

2. Simulation Setup and Material Models

The simulations conducted for this study used the Sandia National Laboratories computational shock and multiphysics code ALEGRA release 8.15.0.[16] Changes in quantities of interest were automated using Dakota,[17] a software tool for uncertainty

quantification, design optimization, calibration, parameter estimation, and sensitivity analysis. Parameterization of individual variables was accomplished by running ALEGRA with Dakota in embedded mode. Running ALEGRA in this manner allows a single high-performance computer (HPC) submission to generate entire series of data from multiple individual simulations.

Simulations were undertaken in an Eulerian framework on a 2-D axisymmetric grid. The Eulerian meshes comprised Cartesian grids of square elements containing 16 elements per millimeter. The radial mesh direction, *r*, extended 30 mm from the axis. The full axial extent of the simulation, *z*, varied depending on the desired flight distance and projectile length from 52 to 72 mm.

All simulations in this study modeled the extrusion of an OFHC Cu projectile through a high-strength steel die. Velocity was the primary Dakota response variable and was measured using a Lagrangian tracer placed one half of an element behind the tip of the projectile. The tracer location within an OFHC Cu sphere passing through a DTE die is illustrated in Fig. 1. In this work, only the foremost tracer was queried by Dakota for velocity.

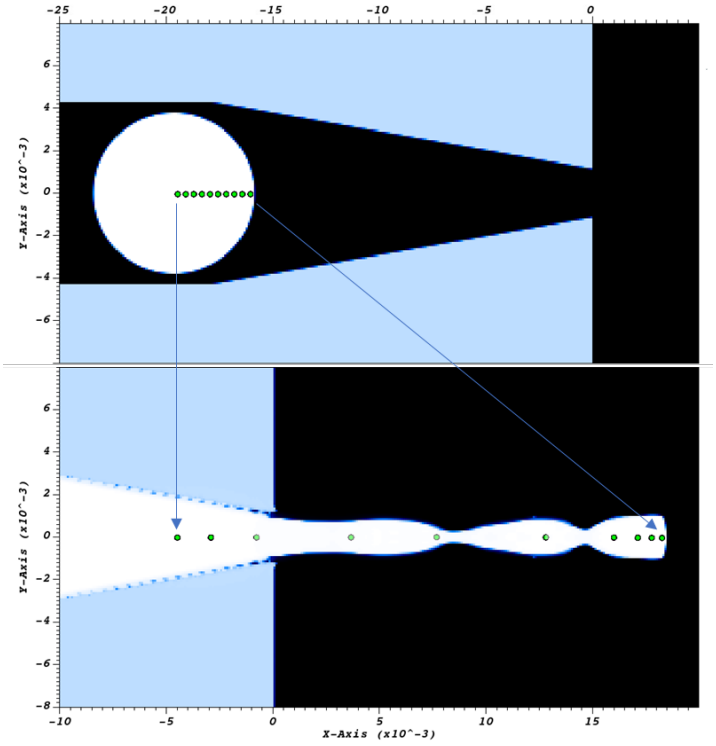

Fig. 1 A magnified portion of a simulation showing an OFHC Cu cylinder approaching a DTE die (top) and the Cu cylinder after passing through the extrusion die (bottom). The foremost tracer (green circle) was used to extract the particle velocity.

In an ALEGRA solid dynamics simulation, each material requires an equation of state (EOS) and a yield model. For the Cu projectiles, MTS was chosen as the yield model. This model is suitable for high strain rates (~10^4 s^{-1}), is capable of capturing both the thermal softening and strain rate hardening of face-centered cubic metals such as Cu, and has parameters available specifically for OFHC Cu in ALEGRA. Furthermore, MTS has shown success reproducing reasonable velocities for a Ta specimen undergoing DTE.[15] Tabular EOS 3337 was chosen for the Cu, and has demonstrated excellent results previously in shaped-charge jet studies.[18] Tabular EOS 2150 was used for the steel die, and JC was chosen for the yield model since parameters for high-strength tool steel are available in the ALEGRA material database.

Published photon Doppler velocimetry data on the DTE velocity of a Cu sphere from Burkett[15] were used to confirm that the chosen material models reasonably reproduced the general trend in velocity enhancement.* The projectile for these simulations was a 7.6-mm-diameter Cu sphere at a temperature of 600 °C, and the conical section of the steel die had a 10° half angle with an exit radius of 2.6 mm. A comparison of the simulated velocities and the experimental velocities for the three highest-velocity cases published in Burkett[15] is shown in Fig. 2.

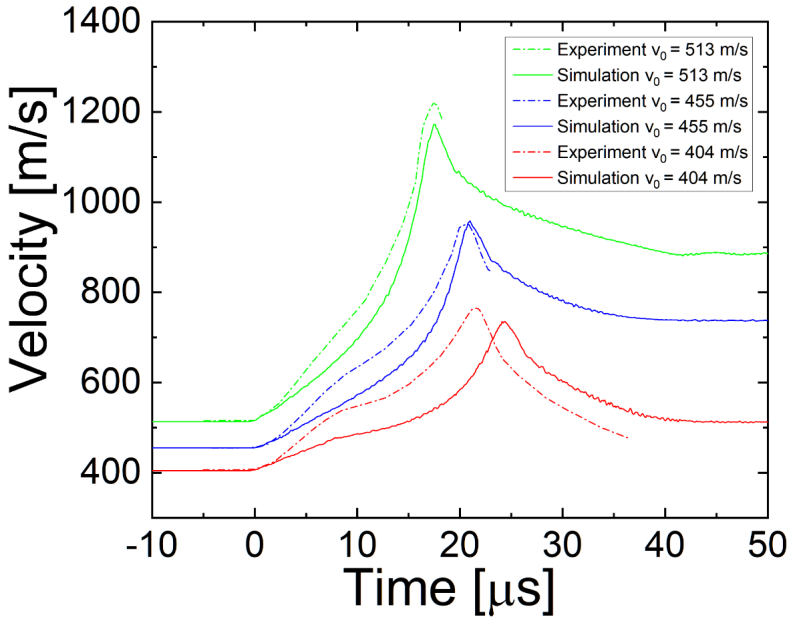

Fig. 2 A comparison of the experimental data from Burkett[15] and ALEGRA simulations showing the temporal evolution of the velocity of a Cu sphere during DTE

* PDV data were provided to Burkett[15] by CP Trujillo.

As indicated in Fig. 2, when the projectile impacts the die, the velocity increases to a maximum and then begins to decease. This decrease has been attributed to "tensile pullback."[7] If the initial velocity is sufficient, the specimen will eventually particulate, and the lead particle will continue in free flight at an elevated velocity. Although some differences exist between simulation and experiment in the temporal evolution of the velocities shown in Fig. 2, for each of the three initial velocities shown there is reasonable agreement for the peak velocity values. The percentage differences in simulated peak velocities from experiment are 3.9%, 0.9%, and 3.8% for initial velocities of 404, 455, and 513 m/s, respectively; thus, the general trend of increasing peak velocities with increasing initial velocities is captured well. Since the peak velocities are reproduced by these simulations with high accuracy, these material models are sufficient for the comparative analysis of DTE component parameters presented here. For the remainder of the report, the simulation of the DTE of the Cu sphere with a 513-m/s initial velocity is used as a reference configuration.

3. Die Variations

Since DTE is a fundamentally straightforward process requiring only that a projectile pass through a conical reducing section of a high-strength die, geometric constraints on the die are few. The two principal geometric features of the die that have an impact on the velocity enhancement that occurs during DTE are the cone apex angle and the exit radius. The influence these parameters have on peak and downrange velocities is examined in this section using ALEGRA. Variations in a third parameter—the exit length—are also considered. The ALEGRA simulations presented here involving the analysis of die features utilized Dakota's vector parameter study method with a continuous design in embedded mode.

The effects of varying the die exit radius and the die half angle on the peak velocities of an extruding 600 °C Cu sphere with an initial velocity of 513 m/s are presented in Fig. 3. A schematic is inset in Fig. 3 depicting the half angle, α, and the exit radius, r_0. Exit radii were decreased from 3.6 to 0.6 mm in 0.2-mm decrements, and half angles were increased from 8° to 14° in 2° increments. In addition, a relatively extreme half angle of 20° was also included. A significant increase in peak velocity for all radii was evident as the half angle increased from 8° to 10°. Generally, for a given half angle, the peak velocity increases with decreasing exit radius. The rate of increase slows significantly at small radii for the 20° half angle in comparison to the others. The simulations show that die material for this widest angle begins to fail at the edges of the exit hole and is deformed slightly outward and downrange ("blown out") as the projectile passes through. This relieves some of the pressure in the specimen and results in a lower peak velocity.

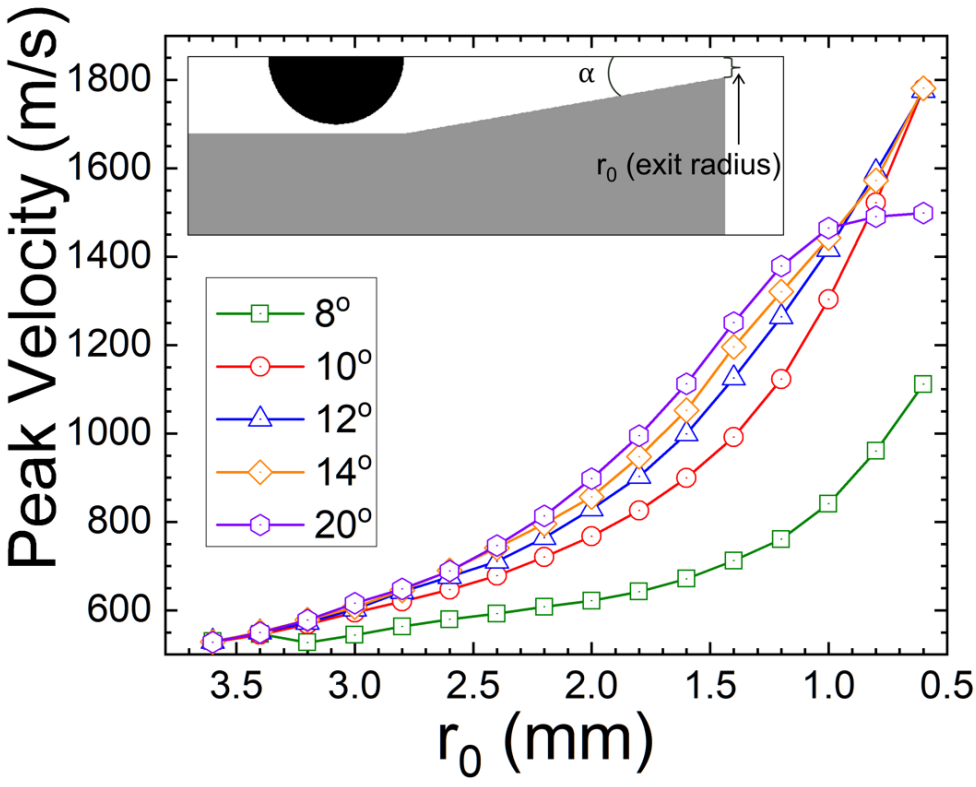

Fig. 3 A comparison of the peak velocity of an extruding Cu specimen for 5 different cone half angles and 16 different exit radii. Inset: a diagram showing the varied dimensions.

In applications where maximizing the velocity of the lead particle is the primary interest, a measurement of the lead particle velocity some distance after it has exited the die is desirable. In this report, the velocity of the lead particle taken 3 cm after it exited the die serves as this measurement and is specified as the "downrange velocity." A spatial location was chosen as a comparison reference because the breakup times of the extruded specimens will vary depending on the die geometry, projectile initial velocity, and projectile temperature.

The downrange velocities of the 600 °C Cu sphere are shown in Fig. 4 for simulations with varying die exit radii and half angles. The initial Cu sphere velocity of 513 m/s is represented on the plot as a dashed black line. Interestingly, the simulations indicate that the threshold at which the DTE of a Cu sphere results in a lead particle with a downrange velocity higher than the initial velocity depends on the die radius and half angle. For wider angles velocity gains were observed at wider radii. For example, the die with the 20° half angle produced a velocity gain for exit radii below approximately 2.6 mm; in contrast, the die with the 8° half angle produced a velocity gain for exit radii below approximately 1.2 mm. Additionally, the impact of the die deformation at small radii for the 20° half angle is also evident in this plot as the downrange velocity decreases below a radius of 1 mm.

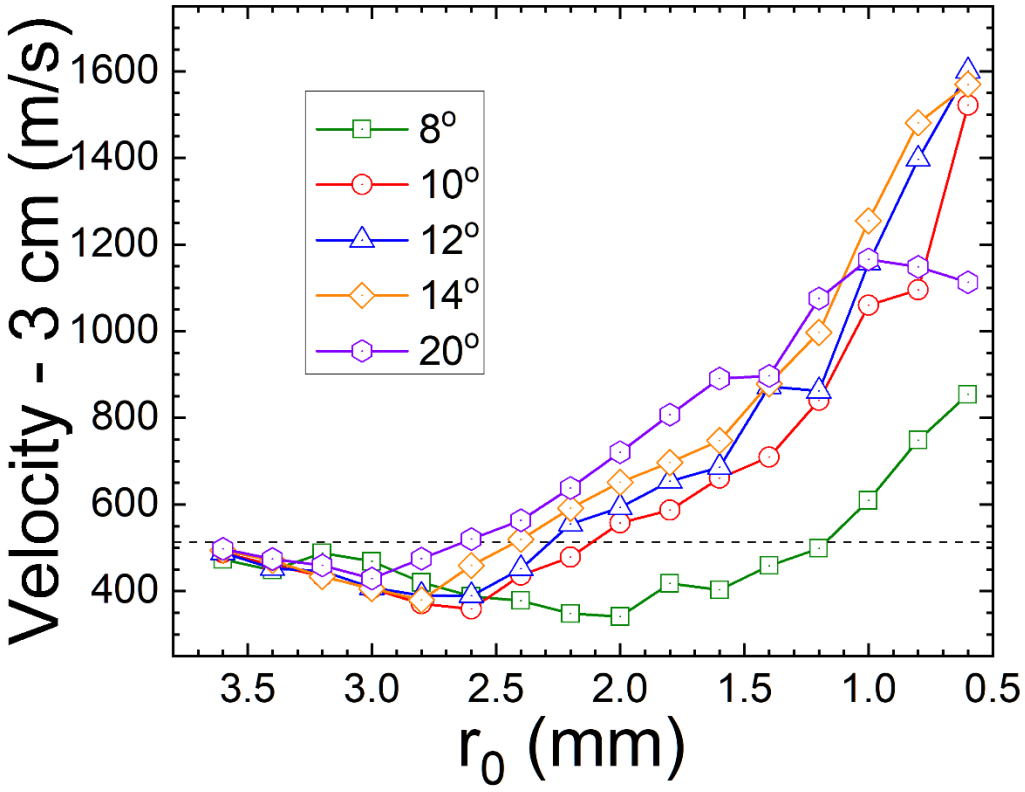

Fig. 4 The velocity of the lead particle of a Cu sphere after DTE measured 3 cm after the die exit for differing exit radii and apex half angles. The horizontal black dashed line indicates the initial velocity (513 m/s) of the Cu sphere.

Not surprisingly, for the half angles considered, simulations indicated that until the radius of the die exit was below approximately 68% of the diameter of the projectile, no downrange velocity increase was observed. For the wider exit radii, although the peak velocity of the lead tracer might have been greater than the initial velocity, the die served as an obstruction that slowed the projectile rather than a device that contributed to a useful increase in velocity.

Another parameter that is of interest from a parametric standpoint is the length of exit channel. For the preceding parametric analysis exploring the half-angle of the cone and the exit radius, it was assumed that the exit radius of the die coincided with a point on the cone with the specified apex half-angle. This geometry results in a minimal volume of die material where the projectile exits the die. That region where a minimal volume of die material interacts with the incoming projectile could result in the fracture or erosion of the die material thereby deleteriously affecting the velocity enhancement. Creating a finite exit channel could alleviate this issue and increase die durability.

Since any modification to a DTE die will impact extrusion dynamics, simulations were conducted to investigate the effects of including an exit channel on the peak and downrange velocities. Topological changes in the extruding specimen with the addition of exit channels were also examined. The lengths of the exit channels inserted in the die varied from 0 to 4 mm in 0.5-mm increments.

The peak velocities, downrange velocities, and lead particle diameters at 3 cm are listed in Table 1. Interestingly, the peak and downrange velocities are lowest for the die without an exit channel. In addition, that die had its largest lead particle diameter when measured 3-cm downrange. Upon close inspection of that simulation, some erosion of die material was observed at the edge of the exit hole. This resulted in the lower velocities and larger particle size. To a lesser extent, these effects were also apparent for the die with the 0.5-mm exit channel. For all other exit channel lengths, the velocities and downrange lead particle diameters are similar with a maximum variation from the highest peak velocity under 2% and a maximum variation from the highest downrange velocity under 8%.

Table 1 Peak velocities, downrange velocities, and lead particle diameters at 3 cm with variations in exit channel length

Exit channel length (mm)	Peak velocity (m/s)	Velocity 3-cm downrange (m/s)	Lead particle diameter 3-cm downrange (mm)
0.0	1176	903	2.0
0.5	1230	949	2.0
1.0	1243	1012	1.9
1.5	1247	940	1.9
2.0	1248	960	1.9
2.5	1250	972	1.9
3.0	1254	1020	1.9
3.5	1258	955	1.9
4.0	1256	1008	1.9

Differences in the topology of three extruding specimens are compared in Fig. 5. The simulation with no exit channel is shown in Fig. 5a, while simulations with exit channels of 2.0 and 4.0 mm are shown in Figs. 5b and 5c, respectively. In Fig. 5c, ℓ represents the dimension that was varied between the simulations. The particulation of the specimen appears to be affected by the inclusion of an exit channel. For example, in comparison to Fig. 5a, a higher number of particles appear to be forming with higher uniformity in the simulations with finite channels.

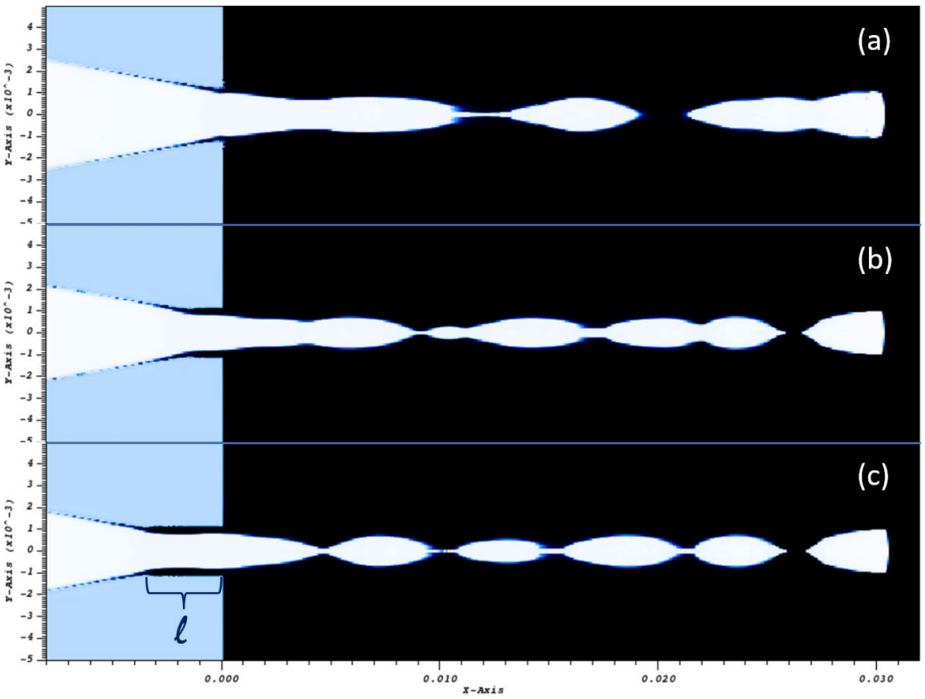

Fig. 5 A comparison of the topology of an extruding Cu specimen approximated 3-cm downrange of the die exit as the exit channel length, ℓ, is varied for (a) 0.0-mm exit channel length, (b) 2.0-mm exit channel length, and (c) 4.0-mm exit channel length

4. Projectile Variations

As shown in Section 3, variations in the geometry of a DTE die can have significant effects on extrusion dynamics. Thus, the role variations in projectile parameters have on the extrusion velocity is a worthwhile investigation. In this section the incoming velocity, temperature, and projectile geometry are examined.

The effects of varying the incoming DTE velocity of a 7.6-mm-diameter Cu sphere at 600 °C on the peak and downrange velocities are first explored. The incoming velocity of the Cu sphere was varied from 400 to 1000 m/s in 50-m/s increments. The results are shown in Fig. 6. Both the peak and downrange velocities increase monotonically. In each case, however, the simulations suggest there are diminishing returns on the percentage increases in velocity with higher incoming velocities. The highest percentage increase in peak velocity was 58.6% and occurred when the initial velocity was at 600 m/s, and the highest percentage increase in downrange velocity was 53.1% and occurred when the initial velocity was at 850 m/s. With increasing velocity, the strain rates also increase, and although the MTS Cu yield model decently reproduces experimental results at 513 m/s and below, confidence in simulation results at higher strain rates would benefit from a similar empirical comparison.

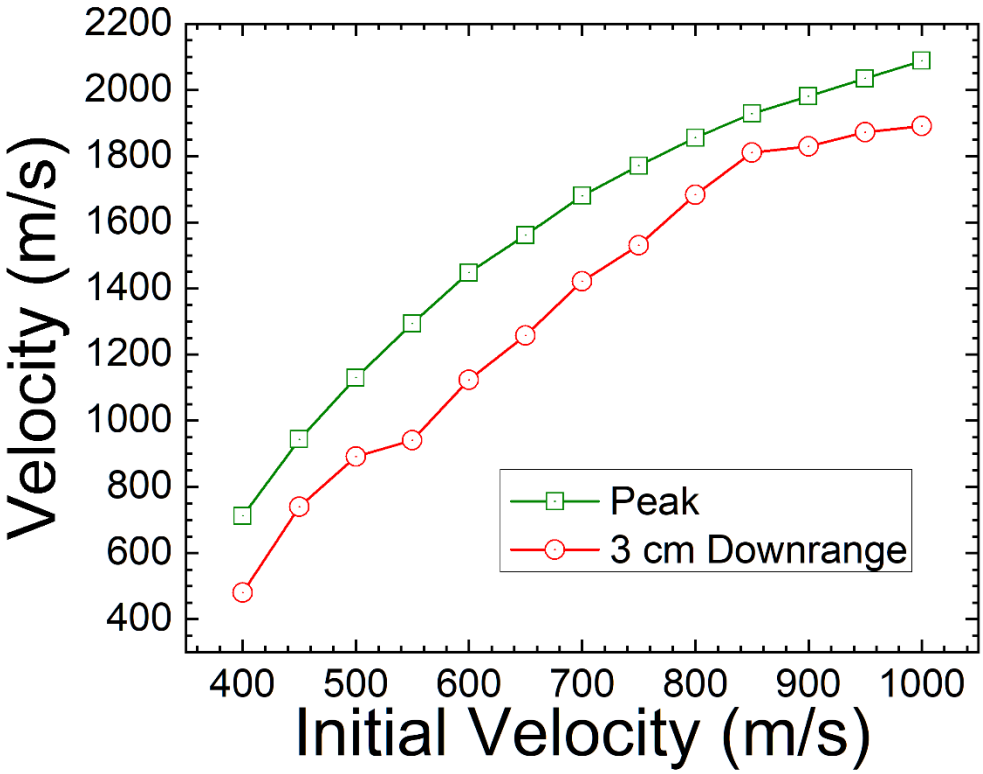

Fig. 6 The dependence of the peak and downrange DTE velocities of a Cu sphere on the initial velocity

Variations in the temperature of the incoming DTE projectile are next examined. The temperature of a 7.6-mm-diameter Cu sphere with an initial velocity of 513 m/s was varied from 400 to 950 °C in 50 °C increments. Note that the final temperature of 950 °C is 135 °C from the melt temperature of Cu at standard atmospheric pressure (1085 °C). Figure 7 shows the velocities from the simulations. The black dashed line again indicates the initial velocity of the Cu sphere. While the peak extrusion velocity increases with increasing temperature, a slight decrease in the downrange velocity was observed around 750 °C. The simulations indicated that as the temperature increases, the projectile breakup time increases as well. The coupling of a more contiguous extruding specimen with changes in other temperature-dependent material parameters could play a role in the decrease of the downrange lead particle velocity. These results suggest that the interplay between temperature-dependent material properties during DTE result in the existence of an optimal temperature for maximizing the downrange velocity of a lead particle.

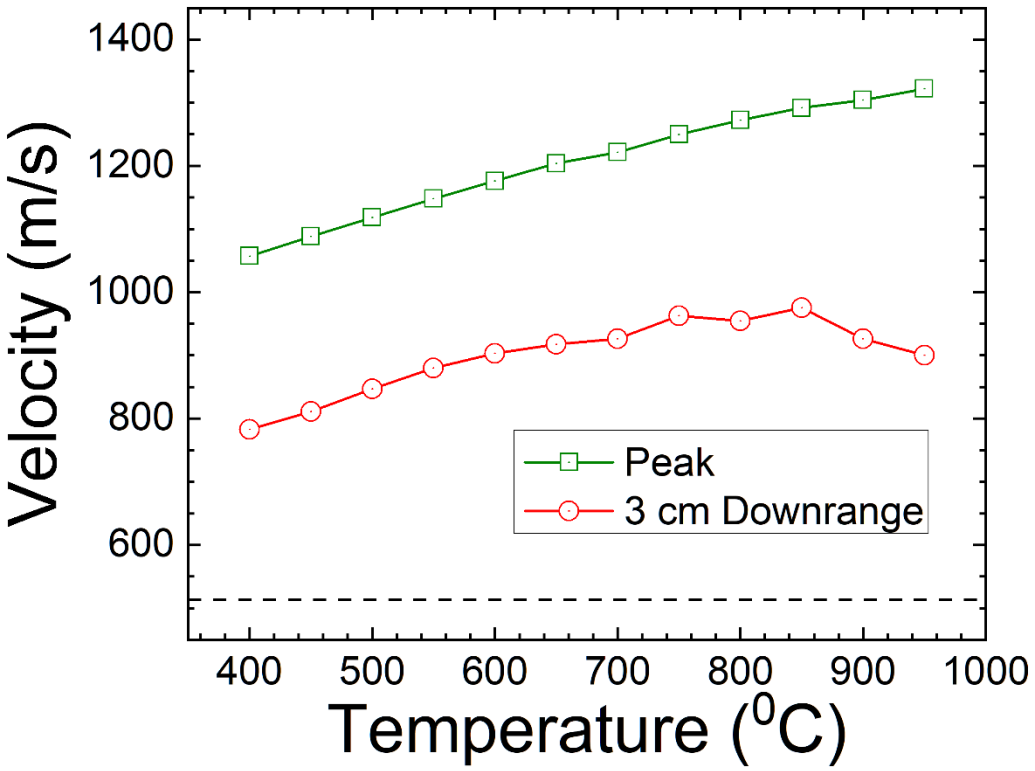

Fig. 7 The effects on peak velocity and the velocity of an extruded projectile 3 cm past the die as the temperature of the projectiles are increased from 400 to 950 °C. The horizontal black dashed line indicates the initial velocity (513 m/s) of the Cu sphere.

The final variation considered in this study involves the geometry of the projectile. Hemispherical projectiles of different masses are compared to the reference case with a spherical projectile. The radius, temperature, and initial velocity of each projectile matched the reference case and were 7.6 mm, 600 °C, and 513 m/s, respectively. Four lengths were considered for the hemispherical nose projectile. The first length was chosen so that the mass of the hemispherical nose projectile would match that of the Cu sphere. The second length was chosen so that the mass of the projectile equaled the mass of a cylinder with a length-to-diameter ratio of one. The final two lengths were 10 and 20 mm.

Figure 8 shows the peak and downrange velocities versus initial kinetic energy for each projectile. Interestingly, the hemispherical nose projectile with a mass matching the sphere had a comparatively lower peak and downrange velocity. Small differences can occur between similar simulations. For example, a difference in mass might arise from the way the material insertion algorithm handles a completely circular shape versus one that has a rectangular feature. A possibility exists, however, that the mass distribution of these two projectiles might also play a role. A focused study on that phenomenon would be required to make that determination with certainty.

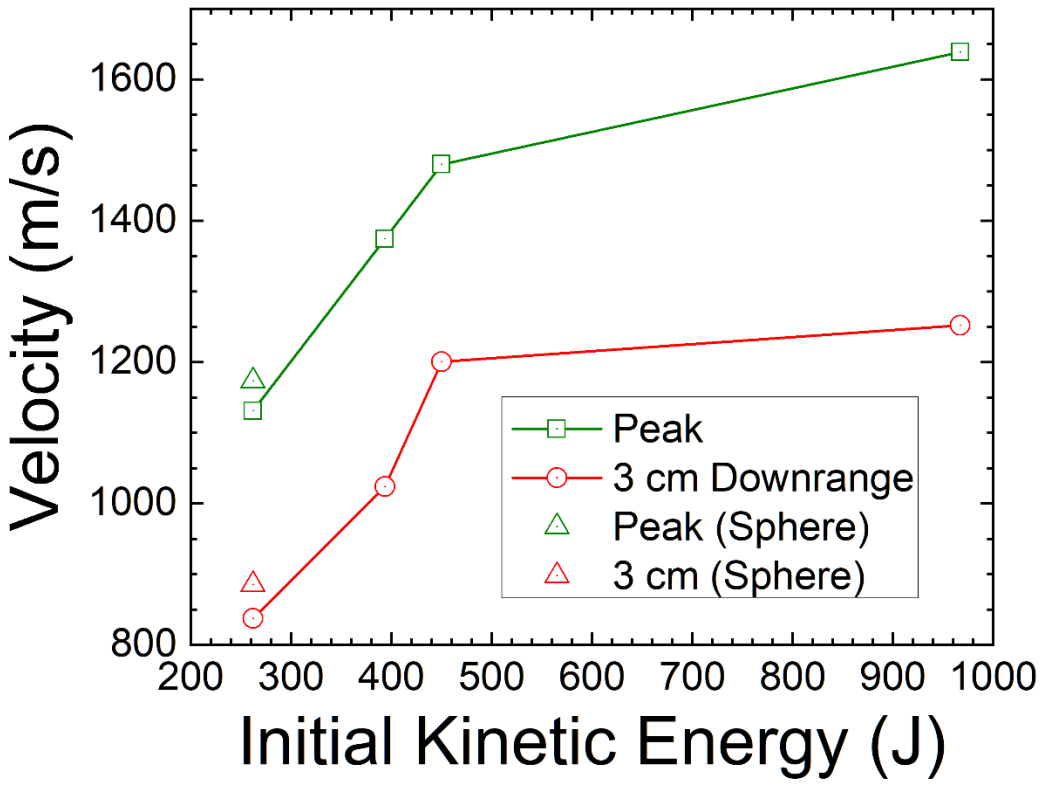

Fig. 8 The effects on peak velocity and the downrange velocity with differing initial kinetic energies for a spherical Cu projectile and hemispherical nose projectiles with varying lengths

Another noteworthy feature in Fig. 8 is the sharp decrease in the percentage increase in both peak and downrange velocities for the hemispherical nose projectile when the kinetic energy increases from 450 (10-mm length) to 967 J (20-mm length). The simulations suggest that when the projectile doubles in length, the downrange velocity percentage increase moves only from 134% to 144%. That corresponds to an increase of approximately 50 m/s. These results indicate that for a given radius and incoming velocity there is an optimum projectile length for maximizing the peak and downrange velocities of a hemispherical nose projectile during DTE.

5. Conclusion

In summary, simulations were conducted exploring parametric changes to a DTE die and to the incident projectile, and several interesting observations have been noted. Peak and downrange velocities were shown to increase as the die half angle increases. Increases in velocity were also observed as the die exit radius was decreased. In addition, introducing an exit channel to a DTE die can affect the topology of an extruding specimen and lead to an increase in downrange velocities.

Even a modest channel of 0.5 mm led to an approximately 5% increase in the downrange velocity.

Variations in the projectile, incoming velocity, temperature, and geometry were also considered. Both the peak and downrange velocities increase with initial velocity. Simulations exploring the temperature and energy variations suggested optimal values may exist that depend on the projectile's incoming velocity, material parameters, and dimensions. The results presented here highlight several potential parametric variations that could be leveraged to increase the velocity of a compact laboratory high-velocity delivery system for material interaction studies.

6. References

1. Bartkowski P, Berning P, Uhlig W, Coppinger MJ. Electrical arc driven hypersonic projectiles. DEVCOM Army Research Laboratory (US); 2019. Report No.: ARL-TR-8683.

2. Uhlig WC, Bartkowski PT, Berning PR, Coppinger MJ. Controlling chamber expansion in miniature electrothermal guns for increased velocity and efficiency. DEVCOM Army Research Laboratory (US); 2019. Report No.: ARL-TR-8722.

3. Uhlig WC, Coppinger MJ, Berning PR, Bartkowski P. Overcoming erroneous erosion of electrically launched projectiles in ALEGRA simulations. DEVCOM Army Research Laboratory (US); 2020. Report No.: ARL-TR-8888.

4. Uhlig WC, Berning PR, Bartkowski PT, Coppinger MJ. Electrically-launched mm-sized hypervelocity projectiles. Int J Impact Eng. 2020;137:103441.

5. Wilmer BL, Uhlig WC, Berning PR, Coppinger MJ. Optimizing performance of compact hypervelocity electrothermal guns: electrode composition and bore diameter. Proceedings of the 2022 Hypervelocity Impact Symposium HVIS; 2022.

6. Gray GT III, Maudlin PJ, Burkett MW, Cerreta EK, Yablinsky CA, Henrie BL, Trujillo CP. Influence of shock prestraining and grain size of the dynamic tensile extrusion response of copper: experiments and modeling. 14th American Physical Society Topical Conference on Shock Compression of Condensed Matter, 2005; Baltimore, MD.

7. Trujillo CP, Martinez DT, Burkett MW, Escobedo JP, Cerreta E, Gray GT III. A novel use of PDV for an integrated small scale test platform. AIP Conference Proceedings; 2012;1426:406–409.

8. Escobedo JP, Cerreta E, Martinez DT, Trujillo CP, Lebensohn RA, Gray GT III. Influence of temperature on the dynamic tensile behavior of zirconium. Metallurg Mater Trans A. 2014 Dec;45a:5877.

9. Coppinger MJ, Wilmer BL, Adams CT, Borys RW Jr. Electrified dynamic tensile extrusion of hemispherical nose aluminum projectiles. DEVCOM Army Research Laboratory (US), 2022. Report No.: ARL-TR-9568.

10. Johnson GR, Cook WH. A constitutive model and data for metals subjected to large strains, high strain rates, and high temperatures. Proceedings of the 7th International Symposium on Ballistics; 1983 Apr 19–21; The Hague, ND. p. 541–547.

11. Rusinek A, Klepaczko JR. Shear testing of a sheet steel at wide range of strain rates and a constitutive relation with strain-rate and temperature dependence of the flow stress. Int J Plasticity. 2001;17(1):87–115.

12. Bonora N, Testa G, Ruggiero A, Iannitti G, Mortazavi N, Hornqvist M. Numerical simulation of dynamic tensile extrusion test of OFHC copper. J Dynamic Behav Matter. 2015;1:136–152.

13. Follansbee PS, Kocks UF. Constitutive description of the deformation of copper based on the use of the mechanical threshold stress as an internal state variable. Acta Metall. 1988;36(1):81–93.

14. Zerilli FJ, Armstrong RW. Dislocation-mechanics-based constitutive relations for material dynamics calculations. J Appl Phys. 1987;61(5):1816.

15. Burkett MW. Eulerian hydrocode modeling of a dynamic tensile extrusion experiment. Proceedings of the 2019 Hypervelocity Impact Symposium; 2019 Apr 14–19; Destin, FL. Paper No.: HVIS2019-057.

16. Robinson AC, Brunner TA, Carroll S, Drake R, Garasi CJ, Gardiner T, Haill T, Hanshaw H, Hensinger D, Labreche D, et al. ALEGRA: an arbitrary Lagrangian-Eulerian multimaterial, multiphysics code. Proceedings of the 46th AIAA Aerospace Sciences Meeting; 2008. Paper No.: AIAA-2008-1235.

17. Adams BM, Bauman LE, William J. Bohnhoff WJ, Dalbey KR, Eddy JP, Ebeida MS, Eldred MS, Hough PD, Hu KT, et al. Dakota, a multilevel parallel object-oriented framework for design optimization, parameter estimation, uncertainty quantification, and sensitivity analysis: version 6.0 user's manual. Sandia National Laboratories (US); 2014. Report No.: SAND2014-4633.

18. Doney RL, Niederhaus JHJ, Fuller TJ, Coppinger MJ. Effects of equations of state and constitutive models on simulating copper shaped charge jets in ALEGRA. Int J Impact Eng. 2020;136.

List of Symbols, Abbreviations, and Acronyms

2-D	two-dimensional
ARL	Army Research Laboratory
Cu	copper
DEVCOM	US Army Combat Capabilities Development Command
DOD	Department of Defense
DTE	dynamic tensile extrusion
EOS	equation of state
HPC	high-performance computer
JC	Johnson–Cook
MTS	mechanical threshold stress
OFHC	oxygen-free high conductivity
Ta	tantalum

1 (PDF) DEFENSE TECHNICAL INFORMATION CTR DTIC OCA

1 (PDF) DEVCOM ARL FCDD RLB CI TECH LIB

1 (PDF) SANDIA NAT LAB J NIEDERHAUS

7 (PDF) DEVCOM ARL FCDD RLA T R FRANCART FCDD RLA TA S BILYK P BERNING M COPPINGER W UHLIG B WILMER FCDD RLA TD R DONEY